Mist/Steam Heat Transfer in Confined Slot Jet Impingement

X. Li

J. L. Gaddis

T. Wang[1]

Department of Mechanical Engineering,
Clemson University,
Clemson, SC 29634-0921

Internal mist/steam blade cooling technology has been considered for the future generation of Advanced Turbine Systems (ATS). Fine water droplets of about 5 μm were carried by steam through a single slot jet onto a heated target surface in a confined channel. Experiments covered Reynolds numbers from 7500 to 25,000 and heat fluxes from 3 to 21 kW/m^2. The experimental results indicate that the cooling is enhanced significantly near the stagnation point by the mist, decreasing to a negligible level at a distance of six jet widths from the stagnation region. Up to 200 percent heat transfer enhancement at the stagnation point was achieved by injecting only ~1.5 percent of mist. The investigation has focused on the effects of wall temperature, mist concentration, and Reynolds number.
[DOI: 10.1115/1.1331536]

Introduction

To improve the overall efficiency of gas turbine engines, the turbine inlet temperature and compressor pressure ratio are continuously increasing for the next generation of gas turbine systems. As a result, even with the potential advancement of future high-temperature materials, highly efficient gas turbine engines are expected to continue to operate at temperatures much higher than the allowable metal temperature of the turbine airfoils, which, in turn, makes effective cooling of the airfoils essential.

With recent adoptions of closed-loop steam cooling by two major gas turbine manufacturers [1,2] for their heavy-frame Advanced Turbine Systems (ATS), a major part of external air-film cooling load will be replaced by internal steam cooling. Generally, the internal heat transfer coefficient is required to be in the range of 8000~10,000 W/m^2 K in order to replace the cooling load currently shared by external air-film cooling. Liquid water can achieve this goal easily, but problems with instability when boiling occurs have discounted its chances. With the availability of steam from the bottom cycle of a heavy-frame ATS, mist/steam cooling has been introduced by this research group [3] as a potential means to enhance the internal cooling effectiveness of turbine airfoils significantly. The advantages and reasons for using mist/steam cooling, a comparison of mist/air and mist/steam cooling, and a review of previous related studies have been presented by Guo et al. [3] and are not repeated here.

Basically, the concept of using mist/steam cooling to enhance cooling effectiveness is based on its following features: (*a*) latent heat of evaporation, (*b*) increased specific heat, (*c*) steeper temperature gradient near the wall, (*d*) lower bulk temperature, (*e*) increased flow mixing induced by steam-particle interactions and particle dynamics, and (*f*) additional momentum and mass transfer induced by evaporation of liquid droplets on/near the wall.

Jet impingement cooling has been applied widely to provide high heat transfer rates in many industrial processes, including the hardening and quenching of metals, tempering of glass, and cooling of electronic components. The early studies show that jet impingement cooling is better than channel cooling for gas turbines, especially for the leading edge of the turbine blades. Single-phase jet impingement has been studied extensively, including heat transfer at the stagnation point, local heat transfer, and effects of turbulence intensity and nozzle geometry. However, few studies have been found on mist jet impingement, including air–water mist and steam–water mist.

Wachters et al. [4] considered the impact of droplets about 60 μm impacting a heated surface in the range of 5 m/s. Impinging droplets could only maintain the spheroidal state with relatively high surface temperatures. The required temperature depended on thermal properties and roughness of the surface as well as the Weber number of the droplets. In the spheroidal state very low rates of heat flow were observed.

Goodyer and Waterston [5] considered mist/air impingement for turbine blade cooling at surface temperatures above 600°C. They suggested that the heat transfer was dominated by partial contact between the droplets and the target surface, during which the droplets vaporized at least partially. A vapor cushion and the elastic deformation of the droplets were responsible for rejecting the droplets. Addition of 6 percent water was found to improve the stagnation point heat transfer by 100 percent, diminishing away from the stagnation point. Droplet size was found to have little effect for 30 μm $< d_{32} <$ 200 μm.

Takagi and Ogasawara [6] studied mist/air heat and mass transfer in a vertical rectangular tube heated on one side. They identified wet-type heat transfer at relatively low temperatures and post-dryout type at higher temperatures. In the wet region the heat transfer coefficient increased with increased heat flux. In the post-dryout region the heat transfer coefficient increased with droplet concentration and flow velocity and with decreased droplet size.

Ganic and Rosenhow [7] studied the effects of dispersed droplets on heat transfer in a gas flow. They demonstrated that the total heat transfer flux is the sum of a single-phase component and a component due to direct impact of the droplets. In trajectory analysis of droplets in the temperature boundary layer, they included a lift term arising from faster evaporation on the side of the droplet nearer the wall where the gas temperature is higher. The higher evaporative rate gives rise to a momentum imbalance equivalent to lift.

Mastanaiah and Ganic [8] conducted experiments on mist/air in the post-dryout region in a vertical circular tube. Performance depended mainly on wall temperature and was independent of the mass velocity for a range of temperatures in film boiling. They confirmed the heat transfer coefficient decreased with increased wall temperature.

Yoshida et al. [9] focused on the effect on turbulent structure with a suspension of 50-μm glass beads. In the impinging jet region, the gas velocity decreased due to the rebound of beads, accompanied by an increase in the normal direction velocity fluc-

[1]Current address: University of New Orleans, New Orleans, LA.

Contributed by the International Gas Turbine Institute and presented at the 45th International Gas Turbine and Aeroengine Congress and Exhibition, Munich, Germany, May 8–11, 2000. Manuscript received by the International Gas Turbine Institute February 2000. Paper No. 2000-GT-221. Review Chair: D. Ballal.

tuations. In the wall-jet region the effect was slight. The Nusselt number was found to increase by a factor of 2.7 for mass flow ratios (solid/gas) of 0.8.

Lee et al. [10] studied the dynamic depositional behavior of droplets in a mist/air flow in a vertical rectangular channel with one side heated. It was found that when the droplet diameter was 30~80 μm, a ''superbly'' effective cooling scheme with ten times the heat transfer enhancement could be established by the evaporation of an ''ultrathin'' liquid film (50~100 μm).

Buyevich and Mankevich [11,12] modeled the particles in the mist as liquid discs separated from the wall by a vapor layer whose thickness is that of the wall roughness. A critical impact velocity was identified to determine whether a droplet rebounds or is captured. They applied the model to dilute mist impingement and reported agreement with experiment.

Fujimoto and Hatta [13] studied deformation and rebound of a water droplet on a high-temperature wall. For Weber numbers of 10–60, they computed the distortions of the droplet as it flattened, contracted, and rebounded. They used a simple heat transfer model to confirm that surface tension dominates vapor production in the rebounding process. Hatta et al. [14] gave correlations of contact time and contact area of the droplet with Weber number.

Guo et al. [3,15] studied the mist/steam flow and heat transfer in a straight tube under highly superheated wall temperatures. Droplet size and distribution were measured by a Phase Doppler Particle Analyzer (PDPA) system. It was found that the heat transfer performance of steam could be significantly improved by adding mist into the main flow. An average enhancement of 100 percent with the highest local heat transfer enhancement of 200 percent was achieved with 5 percent mist. Guo et al. [16] performed an experimental study on mist/steam cooling in a highly heated, horizontal 180 deg tube bend with the same experimental facility as above. Due to the effect of centrifugal force, the outer wall of the test section always exhibited a higher heat transfer enhancement than the inner wall. The highest enhancement occurred at about 45 deg downstream of the inlet of the test section. Only a small number of droplets could survive the 180 deg turn and be present in the downstream straight section. The overall cooling enhancement of the mist/steam flow ranged from 40 to 300 percent with maximum local cooling enhancement being over 800 percent. It increased as the main steam flow increased, but decreased as the wall heat flux increased.

Experimental Facility

Experimental System. The overall experimental system is shown in Fig. 1, which consists of four subsystems: steam system, water system, atomizing system, and test section. The steam system supplies the main steam flow used in the experimental study. The high-pressure (about 8 bar) steam extracted from the steam pipeline existing in the building becomes clean and dry saturated steam after passing through a strainer, a regulatory system, a desuperheater, and a filter tube. The saturated steam at about 1.5 bar then enters the mixing chamber and mixes with the mist from the atomizer system. The mist/steam flow enters the test section through a flexible silicone tube and goes to the condenser, where it is cooled down to water. Water supplies the atomizer (Mee Industries, Inc.) through a high-pressure pump to produce droplets with an average diameter (d_{10}) less than 10 μm at 68 bar. Any extra water in the mixer goes to drain through a steam trap. The arrangement of nozzles in the mixer has an important effect on the mist/steam flow. Four nozzles are connected by two valves to allow one, three, or four to operate together.

The test section is designed to implement heat transfer measurement as well as optical penetration. It consists of a single slot jet, heaters, thermocouples, and optical windows. Figure 2 shows the layout of this test section. A tube 25 mm in diameter and 125 mm long connects the 50 mm flexible tube to the settling chamber, which is 70 × 100 mm in cross section and 60 mm long. The

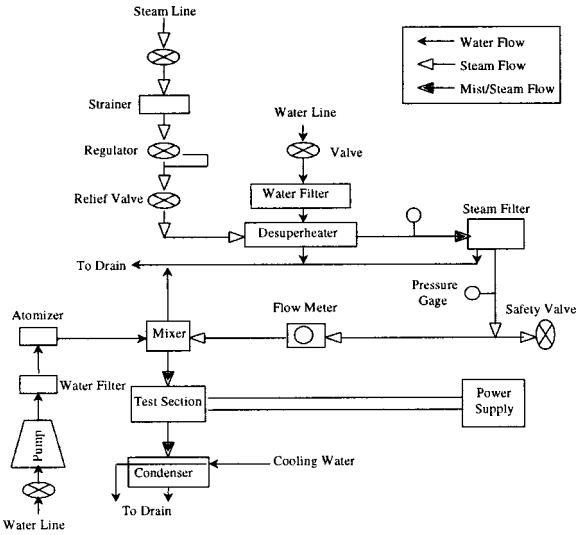

Fig. 1 Schematic of experimental system

collecting pipes are at both ends. The whole test section slides horizontally and moves vertically by insertion of shims. Flexible silicone rubber tubes are used to connect the test section with the mixer and the condenser to implement movement in both directions. The container is made of aluminum to reduce the total weight and assembled by bolts. Based on other studies and the recommendations from industry and limited by the steam-line capability, the rounded-entrance slot size is 7.5 × 100 mm with a nozzle-to-target spacing of 22.5 mm. The channel length is 250 mm. This size of slot jet gives a Reynolds number of about 25,000 with a jet velocity of about 30 m/s. Droplets with very high velocity may damage the heated surface, especially for a long period of operation. Therefore, the jet used in this study is scaled up from the industrial application to achieve the current Reynolds number. On the plus side, these dimensions are convenient for optical measurement.

To cover more extensive areas and prevent overheating, five discrete heater elements are used. The segmented heated surface is mounted firmly to a backup plate of high temperature and low thermal conductivity. The middle one, which covers the stagnation point, is only the half width of the other four identical elements (38 × 76 mm). Five heater elements are in series electri-

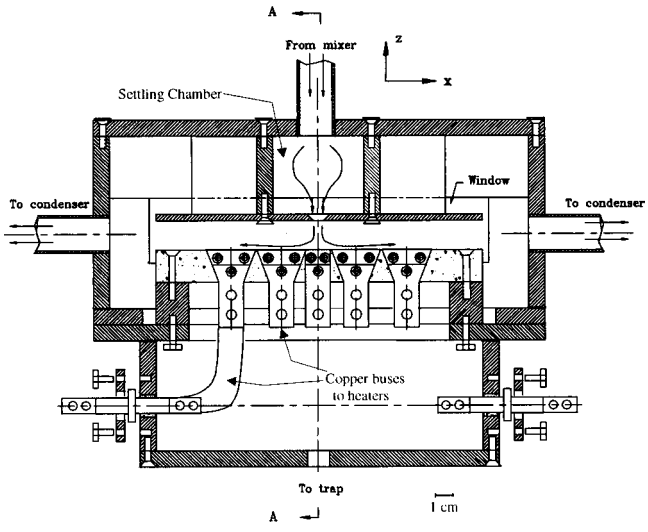

Fig. 2 Design of test section

cally. Stainless steel sheet (Type 316), with a thickness of 0.4 mm, is used for the four larger elements. The center element is copper nickel with one-fourth the electrical resistivity of stainless steel. This yields an approximately constant heat flux within 10 percent.

Two large, flat Pyrex windows are used to cover the whole side-confining wall of the channel. Such big windows make the optical measurement easier and the direct examination on the condition of heated surface possible. The data at different locations can be obtained by moving the test section or the optical system. Compared with moving the jet issuing plate while a small window is used, this scheme can always make a symmetric flow condition and cause little sealing problem. O-rings are used to seal the optical windows.

The test section is directly heated by a DC power supply, which has a maximum voltage of 7 V and a maximum current of 750 A. To maintain a dry and clean window, hot air (200°C) from an auxiliary heater is used to heat the window.

Experimental Instrumentation

Droplet Measurement. The droplet measurement is conducted by a Phase Doppler Particle Analyzer (PDPA). Two laser beams (488 nm, green) with a waist diameter of 0.115 mm are issued from the transmitter and focused on the same region, which generate the fringes for the PDPA system. The PDPA receiver and analysis software (Aerometrics) produce data on velocity parallel to the heater surface, droplet size distribution, and droplet count rate. The PDPA system is fixed; different measurement locations are achieved by moving the test section.

Temperature Measurement. All temperatures are measured by Omega 30-gage (wire diameter about 0.25 mm) Chromega/Alomega (K type) thermocouples with braided fiberglass insulation. A data logger (FLUKE Model 2250) is used to monitor and record the temperature. The thermocouples, along with the data logger, were calibrated against a standard Resistance Temperature Device (RTD) system for nominal temperature uncertainty of 0.3°C. To measure the temperature distribution on the heated surface, thermocouples are strategically placed at the stagnation point and at about 1, 2, 3, 5, 8, and 11 slot widths away from the jet center. Only half of the heated surface is measured, while a single thermocouple at the other side is placed to check for symmetry. The temperature at the inlet of the test section and the temperature of water for the atomizer are also measured.

Flow Rate and Others. Steam flow rate is measured by an orifice flow meter. The catch-and-weigh method is also used to measure the flow rates and calibrate the flow meter in-situ. Water flow from the trap under the mixer is essential to determine the water concentration in the mist. The water flow rates from the traps just before the test section and at the bottom of the test section are also measured. The water flow rate to the atomizer can be adjusted by changing the pump pressure.

The heating power to the test section is obtained from the current and the voltage across the test section. The current is given by the voltage across the precision shunt (with a resistance of $1.333 \times 10^{-4}\ \Omega$) of the power supply. The voltage across the test section is measured directly by a voltmeter. Pressure gages before and after the steam filter indicate the pressure of the steam.

Data Reduction and Uncertainty Analysis

Heat Transfer Coefficient. For jet impingement, the heat transfer coefficient is usually defined as

$$h(x) = \frac{q''(x)}{T_w(x) - T_j} \tag{1}$$

where q'' is the wall heat flux, T_w is the local wall temperature, and T_j is the jet temperature. The steam saturation temperature is taken as the jet temperature for the current study. The wall temperatures are measured by thermocouples electrically insulated by mica at the back of the heater. Since the temperature drop across the heater is less than 0.5°C, which is negligible compared with $(T_w - T_j)$, the temperatures of the thermocouples are used as the wall temperatures.

The heat flux on the heater can be obtained from the heating power divided by the heating area, assuming the heater has a uniform thickness. In fact, the heating power can be obtained directly from the electrical resistance of the heater components and the current passing through the heater as follows:

$$q'' = I^2 \xi / \delta B^2 \tag{2}$$

where I is the current passing through the heater and ξ is the resistivity of the heater materials. δ and B are the heater thickness and width, respectively. Calculation by this equation avoids measurement error of the heater length and of the voltage across the test section due to contact resistance. In the current design, the supporting block for the heaters is ceramic with low heat conductivity and it is surrounded by saturated steam. A simple one-dimensional heat conduction model is used to provide a correction of back heat loss less than 5 percent in data processing.

Flow Parameters. Steam traps in the mixer, immediately upstream of the test section and from the condenser, allow determination of average liquid flow in the test section. The velocity and size of the droplets are given directly by the PDPA system. The concentration of the liquid phase can be found from the droplet average diameter, d_{30}, and the data rate (n) of the PDPA system:

$$m_l = \frac{\pi}{6} \rho_l d_{30}^3 n \tag{3}$$

In our experiment there appears to be frequent interruption of the signal by droplets on the glass. Thus, the value of n is taken as the largest value of many observations. The liquid concentration obtained by the PDPA system is usually smaller than that obtained by the balance of flow rates.

Uncertainty Analysis. Based on the methodology developed by Moffat [17], the nth-order uncertainty analysis is conducted on both heat transfer and flow rate in this study. The results of uncertainty analysis are summarized in Table 1. It is found that the uncertainty for heat transfer is about 5~7 percent and the largest source is the heating voltage of the power supply. For the flow rate, although the uncertainty for the steam phase is very small, the mist concentration has a large uncertainty, about 40 percent, and the largest source is Δt (sampling time). The main sources for the uncertainty of Reynolds number are the steam viscosity, μ_s, and the slot length. The uncertainty of Reynolds number is not large either. The detailed uncertainty analysis is documented by Li [18].

Table 1 Results of uncertainty analysis

Resultants	Nominal Value	Nth-order Uncertainty (%)	Largest Source
m_l/m_s	2.43×10^{-2}	19.3	Δt
Re	15300	1.65	μ_s
q″	13.4 (kW/m^2)	5.43	V_{shunt}
h	268 (W/m^{2}K)	6.27	V_{shunt}
Nu	161	6.50	V_{shunt}

Experimental Results and Discussions

Preliminary Experiments and System Verification. Preliminary studies on single-phase steam jet impingement were conducted first to verify that the whole experiment system was reliable. The results also serve as a baseline for mist/steam jet impingement. Different heat fluxes as well as different jet veloci-

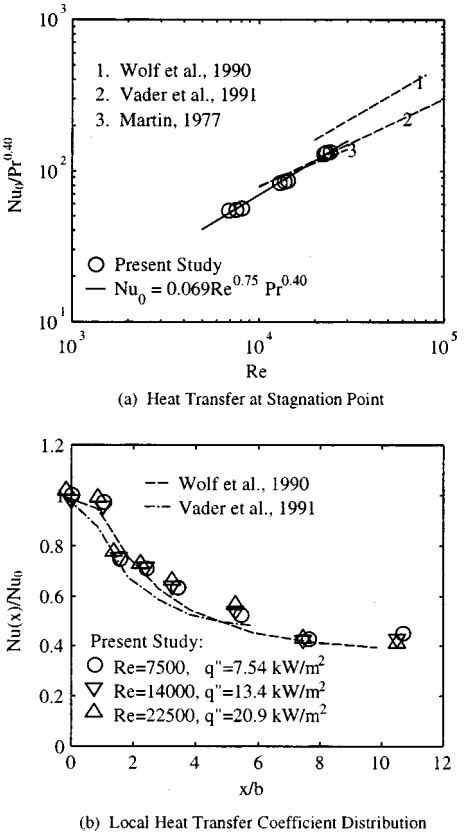

Fig. 3 Heat transfer results for steam-only flow

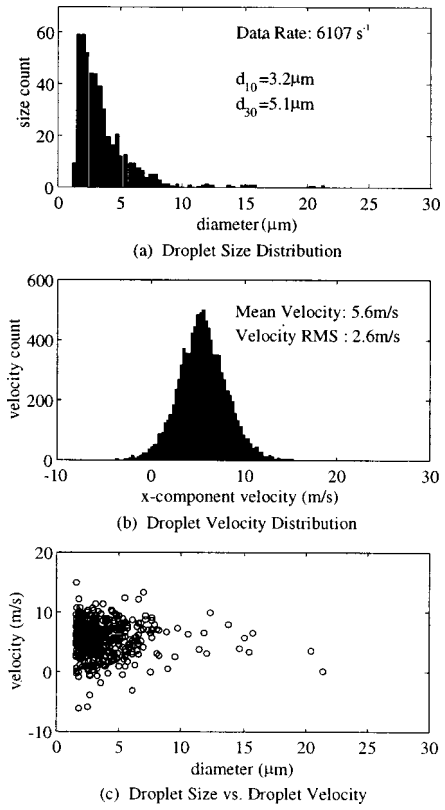

Fig. 4 A typical result of PDPA measurement with one nozzle at Re=15,000, $x/b=2$, and $z/b=0.5$

ties have been tested. Figure 3(*a*) shows the heat transfer results at the stagnation point. The following correlation can be used to represent the data at the stagnation point:

$$\mathrm{Nu}_0 = 0.069\ \mathrm{Re}^{0.75}\ \mathrm{Pr}^{0.40} \tag{4}$$

The characteristic scale used in the Reynolds number and Nusselt number is $2b$, two times the slot width. Figure 3(*b*) shows the distribution of local heat transfer coefficient. The present results are in basic agreement with prior studies. The power of the Reynolds number in Eq. (4) is higher than in other studies due to the narrow range of Reynolds number. In fact, the heat transfer results for jet impingement are subject to variations because of different nozzle designs, different heated surface condition, target distances, and different turbulence intensity. The power for Reynolds number can range from 0.5 to 0.8 [19]. Since the present study does not focus on the effect of different flow parameters and different configurations but only on the effect of water droplets on heat transfer, the steam-only tests support that this experiment system is reliable without large bias error sources.

The symmetric character of the flow was examined by both temperature and velocity measurements. The measurement results, including both steam-only flow and mist/steam flow, indicate, though not shown, that the flow is highly symmetric.

Two-Phase Mist/Steam Jet Impingement

Results of Droplet Measurement for a Typical Case. With the experimental system proven by preliminary studies, the typical behavior of mist/steam jet impingement is examined. The Reynolds number is 15,000 and the heat flux is 13.4 kW/m^2. Figure 4 shows the typical distributions of the droplet size and *x*-component velocity obtained by the PDPA system at a specific location close to the stagnation region ($x/b=2$ and $z/b=0.5$). The droplet size ranges from 1 to 15 μm with an arithmetic average diameter of 3.2 μm. The velocity of the droplet has a large range from -2 to 12 m/s with an average value of 5.6 m/s, which is due to the high turbulence of the shear layer in a jet impingement flow. It can also be seen that the droplet size does not have a close relationship with the droplet velocity, which suggests the droplets follow the main flow well. The distribution of the average droplet size obtained at different locations throughout the test section indicates that the droplet size remains the same at all locations except for the region close to the heated surface, where the droplets become smaller along the wall because of evaporation.

Liquid Concentration Measurement. By using both the catch-and-weigh method and the PDPA data, liquid flow rate was measured for different steam flow rates and with different numbers of nozzles. The results are listed in Table 2. The data range indicates the measurement uncertainty. The liquid concentration was found to decrease with the main flow rate. It was believed initially that a higher steam flow rate would transport more liquid. However, further study found that the liquid flow rate itself decreases with increasing steam flow rate. The possible reason is that high-velocity agitation of mist and steam in the mixer makes more droplets hit the wall and drain out.

More nozzles produce higher liquid concentration, which is also indicated by heat transfer measurements. Direct observation found that liquid streams along the unheated walls, which means some of the liquid collected by catch-and-weigh does not affect the heated surface and the true liquid concentration in the main

Table 2 Results of liquid concentration measurement

Reynolds Number of Steam-Only Flow	Mist Concentration (%)		
	One Nozzle	Three Nozzles	Four Nozzles
7500	3.0~4.0	6.0~8.0	8.0~10.0
15000	1.0~2.0	2.0~3.5	3.0~4.5
22500	0.5~1.0	1.0~1.5	1.5~2.0

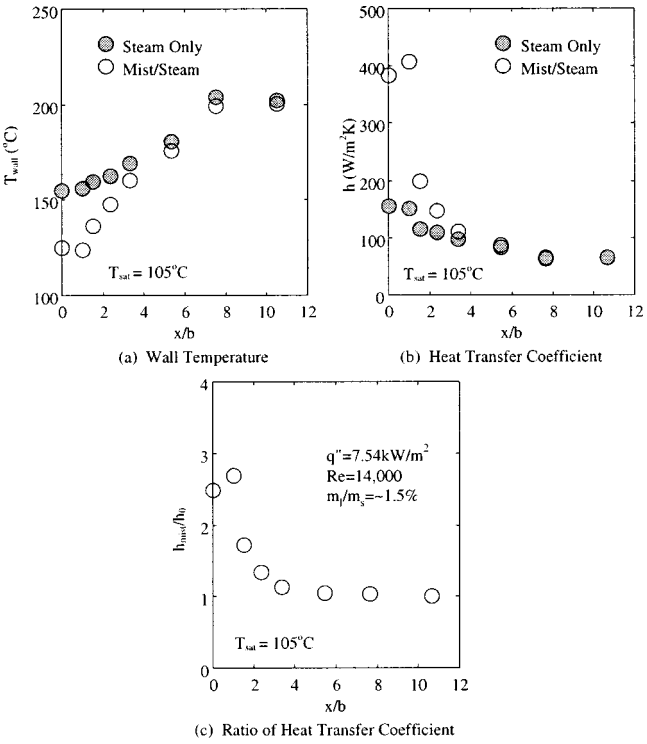

Fig. 5 A typical heat transfer result of mist/steam jet impingement (q''=7.54 kW/m², Re=14,000 and m_l/m_s=~1.5 percent)

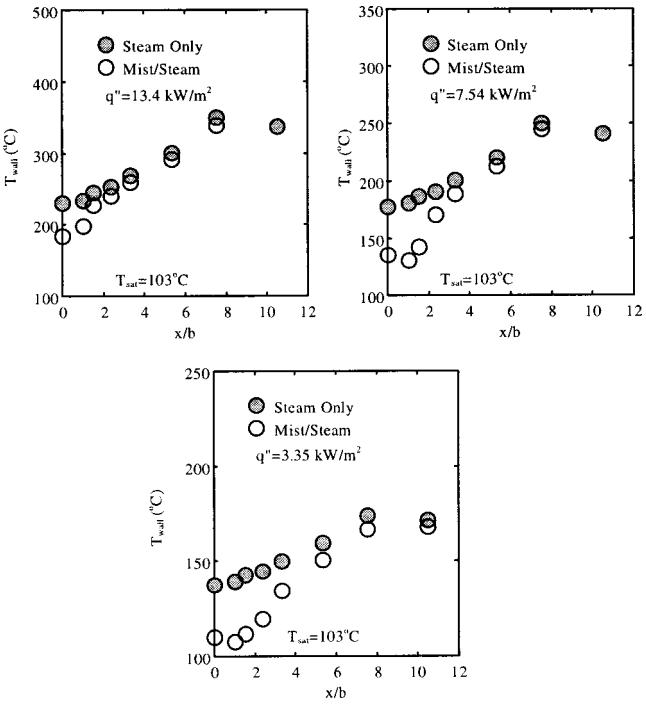

Fig. 6 Wall temperature distribution at different heat fluxes (Re=7500 and m_l/m_s=~3.5 percent)

flow is lower than the calculated value. This effect, varying with the main flow rate, can be used to explain partially the lower value given by the PDPA method.

Results of Heat Transfer for a Typical Case. With a Reynolds number of 14,000 and a heat flux of 7.54 kW/m², the typical heat transfer performance of mist/steam jet impingement cooling is summarized as shown in Fig. 5. In Fig. 5(*a*) the temperature distribution with mist is compared to that without mist, showing clearly the depression in temperatures caused by the mist. The heat transfer coefficient calculated by Eq. (1), as shown in Fig. 5(*b*), is considerably larger near the stagnation point. For $x/b < 2$ the mist effect is strong, declining to about $x/b = 6$ where it becomes negligible. Figure 5(*c*) shows the enhancement, which is the ratio of mist to dry heat transfer coefficient of Fig. 5(*b*). The enhancement for this typical case is 150 percent for ~1.5 percent mist content at the referenced conditions. The mist effect is depressed at the centerline compared with $x/b = 1$, attributed to the divergence of path lines resulting in defocusing of the mist together with the existence of droplet rebound and multiple contacts.

The reduction in enhancement downstream could be due to lack of survival of droplets past the stagnation point or because the droplets become thermally remote from the wall. In this case, as is typical, only a small fraction of the droplets must be evaporated to account for the heat transfer in the stagnation region. Therefore the droplets do survive, a fact corroborated by the PDPA surveys in the downstream region. Therefore the only plausible reason for negligible enhancement for $x/b > 6$ is that the droplets have become thermally remote. This contrasts with the observations of Guo [15] in a straight tube, where the mist always maintained a 10 to 20 percent enhancement even far downstream.

An extensive study has been performed by Li [18] to model the dynamics of liquid droplets impinging on a hot surface and transported in the boundary layer. Only a brief summary is given here. A study of the droplet trajectory shows the droplet has little time to evaporate inside the boundary layer. Near the stagnation point, assuming an elastic rebound at expected velocities, the exposure to superheated vapor causes about 0.1 percent of the liquid mass to evaporate. Therefore, it is deduced that most of the heat transfer enhancement is caused by other mechanisms. One possible mechanism would be the direct heat transfer from wall to droplet. Some of the droplets may be captured on the wall for a short time before they rebound, especially at low wall temperature. The in-

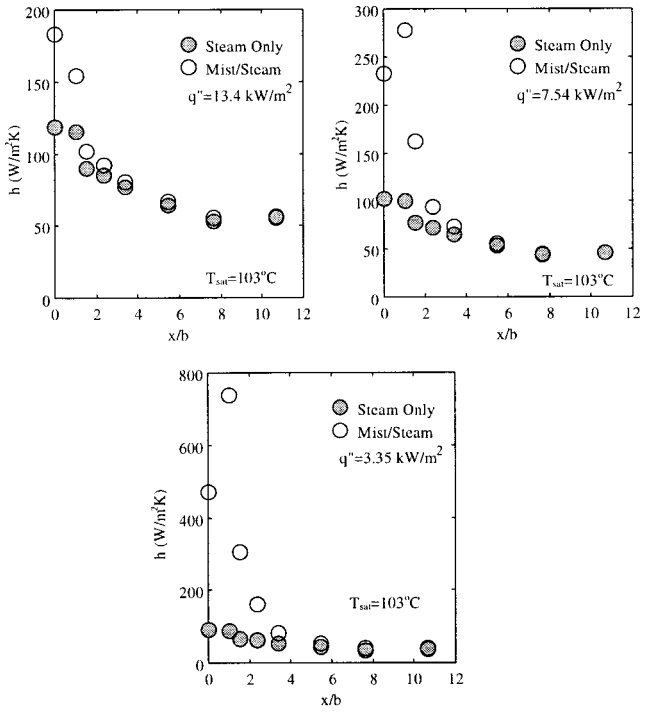

Fig. 7 Heat transfer coefficient at different heat fluxes (Re=7500 and m_l/m_s=~3.5 percent)

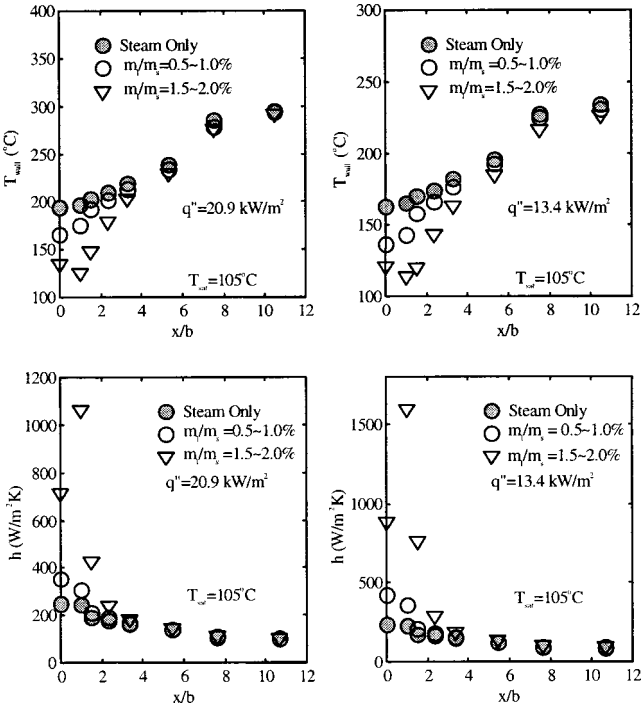

Fig. 8 Effect of liquid concentration on wall temperature and heat transfer coefficient at Re=22,500 and different heat fluxes

creased mixing and turbulence in the boundary layer due to the droplet injection may also contribute to the enhanced heat transfer. This can be supported by the experimental studies on single-phase flow with solid particles inside [9,20].

Effect of Target Wall Temperature on Heat Transfer. The wall temperature plays an important role in the mist heat transfer. The droplets are slowed as they approach the wall and are acted on by the evaporative lift force. As they penetrate the boundary layer and contact the wall, the droplets are expected to deform, as suggested by Hatta et al. [14] for a time dependent on the wall temperature. At low enough temperatures, the droplets could wet the wall and evaporate completely, while for higher temperatures the droplet will overcome any subcooling associated with the pressure of deformation, form vapor, and be repelled from the wall. Direct observation of the surface at all heat fluxes showed no evidence of droplet residence or any accumulated film. The complicated phenomenon noted by Guo et al. [15] resulted from a pre-existing liquid film and is not relevant here. The downstream region of Guo's observation is more comparable. In the present study, data with several heat fluxes are available to examine the temperature effect. Figure 6 shows the temperature distributions under different heat fluxes. Figure 7 shows the corresponding heat transfer coefficient. The variation in single-phase heat transfer coefficient produces a constant Nu using the conductivity evaluated midway between wall and saturation temperature. The stagnation point heat transfer is enhanced by 40 percent at high heat flux, $q''=13.4$ kW/m^2 and the enhancement increases to over 400 percent at low heat flux, $q''=3.35$ kW/m^2. Similar results about the effect of the wall temperature on two-phase heat transfer were reported by Guo et al. [15] and Takagi and Ogasawara [6].

Effect of Liquid Concentration on Heat Transfer. Figure 8 shows results obtained with different liquid concentrations. As expected, increasing the liquid content significantly improves the heat transfer performance. The enhancement can rise to higher than 300 percent from 80 percent when the liquid content increases to 1.5~2.0 percent from 0.5~1.0 percent for Re =22,500 and $q''=20.9$ kW/m^2. However, increasing liquid content does little to improve the heat transfer far away from the stagnation point.

Effect of Steam Flow Rate on Heat Transfer. A high steam flow rate, which means high jet velocity in the present study, will force more droplets to approach the wall. Therefore, more heat can be removed by mist if the mist concentration is the same. However, since the single-phase heat transfer also increases with the main flow rate, the enhancement ratio of the heat transfer coefficient is more complicated. Because the liquid content depends on the main flow rate, it is very difficult to control the experiment under identical liquid concentration and different Reynolds number, although a different number of nozzles can be used. Based on the limited data, it is found that the enhancement ratio is proportional to $Re^{0.3}$ at $T_w=200$°C, which means that increasing the main flow rate will improve the heat transfer enhancement. Guo et al. [15] gave a similar conclusion based on mist/steam cooling in a straight pipe.

Relevance to Turbine Applications. Actual application is expected at 25~35 bar, and Reynolds number to 400,000. Projections to the higher Reynolds numbers of gas turbine applications will increase the single-phase heat component and improve the mist component, based on the trends herein. At the increased wall superheat values, which may reach 700°C, there may be a decline in the mist effect. But the trends indicate that the mist concentration continues to influence the mist effect and it is expected that the higher fluid density will permit carrying increased mist concentration. More study will be required to establish whether higher pressures and temperatures will support useful mist enhancement.

Conclusions

A heat transfer enhancement has been observed due to mist added to steam in an impingement flow. A 150 percent enhancement with a mist concentration of 1.5 percent is typical in the stagnation region. The highest effect is in the stagnation region $x/b<2$, where b is the slot width. From $x/b=2$ to $x/b=6$ the effect wanes, and for $x/b>6$ there is no significant effect. The stagnation point enhancement is strongly influenced by heat flux, increasing from 40 percent at the highest flux to over 400 percent as the flux is reduced by a factor of four. The increase in enhancement is roughly proportional to the liquid content at the stagnation point, but positions downstream remain unaffected at any liquid rate. The heat transfer enhancement is modestly affected by steam velocity (Reynolds number). Tentatively the enhancement varies with $Re^{0.3}$, based on limited data. For low heat flux and high liquid flow conditions the maximum cooling effect is located away from the stagnation point.

Mechanisms noted include the systematically dry condition of the heated surface, having neither film nor visible droplets for long enough to be seen by eye. Calculations of droplet trajectory and thermal boundary layer indicate the droplets have too little residence time to evaporate significantly. The PDPA data indicate relatively large ranges of velocity parallel to the heater surface. Surveys downstream on the plate do indicate smaller droplets near the heated wall, but no elevation in concentration. Estimates suggest that the direct contact heating of droplets is responsible for most of the enhancement, consistent with these observations. Few or no droplets evaporate completely.

Acknowledgments

The authors would like to thank Graver Separations (Wilmington, DE) for donating the steam filters for the experiment. We also want to thank Mee Industries, Inc. (El Monte, CA) for donating the pressure atomizers and the high-pressure pump. We appreciate the help from Dr. T. Guo in setting up the test facility. This

research was sponsored by the U.S. Department of Energy under contract No. DOE/AGTSR 95-01-SR-034, and was managed by Dr. N. Holcombe at the Federal Energy Technology Center and by Dr. Larry Golan at the South Carolina Institute for Energy Studies.

Nomenclature

B = width of heat element
b = jet width=7.5 mm
d = diameter of droplet
d_{10} = arithmetic mean diameter
d_{30} = volume mean diameter
d_{32} = Sauter mean diameter
h = heat transfer coefficient
I = current through the heater
k = thermal conductivity of vapor
m = mass flow rate
Nu = Nusselt number=$h2b/k$
n = data rate, s^{-1}
Pr = Prandtl number
q'' = heat flux
Re = Reynolds number=$\rho_s V_j 2b/\mu_s$
T = temperature
t = time
V_j = average jet velocity at jet exit
V_{shunt} = voltage cross the shunt
x = coordinate along the target wall
z = coordinate along the jet centerline
δ = thickness of heater elements
μ = dynamic viscosity
ρ = density
ξ = resistivity, Ωm

Subscripts

0 = stagnation point
j = jet
l = liquid phase
s = steam
sat = saturated
w = wall

References

[1] Bannister, R. L., and Little, D. A., 1993, ''Development of Advanced Gas Turbine System,'' *Proc. Joint Contractor Meeting: FE/EE Advanced Turbine System Conference; FE Fuel Cells and Coal-Fired Heat Engine Conference,* Aug., Morgantown, WV, pp. 3–15.
[2] Mukavetz, D. W., 1994, ''Advanced Turbine System (ATS) Turbine Modification for Coal and Biomass Fuels,'' in: *Proc. Advanced Turbine System Annual Program Review Meeting*, Nov. 9–11, ORNL/Arlington, VA, pp. 91–95.
[3] Guo, T., Wang, T., and Gaddis, J. L., 2000, ''Mist/Steam Cooling in a Heated Horizontal Tube: Part 1 — Experimental System,'' ASME J. Turbomach., **122**, pp. 360–365.
[4] Wachters, L. H. J., Smulders, L., Vermeulen, J. R., and Kleiweg, H. C., 1966, ''The Heat Transfer From a Hot Wall to Impinging Mist Droplets in the Spheroidal State,'' Chem. Eng. Sci., **21**, pp. 1231–1238.
[5] Goodyer, M. J., and Waterston, R. M., 1973, ''Mist-Cooled Turbines,'' *Proc. Conf. Heat and Fluid Flow in Steam and Gas Turbine Plant*, IMechE, pp. 166–174.
[6] Takagi, T., and Ogasawara, M., 1974, ''Some Characteristics of Heat and Mass Transfer in Binary Mist Flow,'' *Proc. 5th Int. Heat Transfer Conf*., Tokyo, pp. 350–354.
[7] Ganic, E. N., and Rohsenow, W. M., 1973, ''Dispersed Flow Heat Transfer,'' Int. J. Heat Mass Transf. **20**, pp. 885–866.
[8] Mastanaiah, K., and Ganic, E. N., 1981, ''Heat Transfer in Two-Component Dispersed Flow,'' ASME J. Heat Transfer, **103**, pp. 300–306.
[9] Yoshida, H., Suenaga, K., and Echigo, R., 1988, ''Turbulence Structure and Heat Transfer of a Two-Dimensional Impinging Jet With Gas–Solid Suspensions,'' ASME HTD-Vol. 2, pp. 461–467.
[10] Lee, S. L., Yang, Z. H., and Hsyua, Y., 1994, ''Cooling of a Heated Surface by Mist Flow,'' ASME J. Heat Transfer, **116**, pp. 167–172.
[11] Buyevich, Yu. A., and Mankevich, V. N., 1995, ''Interaction of Dilute Mist Flow With a Hot Body,'' Int. J. Heat Mass Transf., **38**, pp. 731–744.
[12] Buyevich, Yu. A., and Mankevich, V. N., 1996, ''Cooling of a Superheated Surface With a Jet Mist Flow,'' Int. J. Heat Mass Transf., **39**, pp. 2353–2362.
[13] Fujimoto, H., and Hatta, N., 1996, ''Deformation and Rebounding Processes of a Water Droplet Impinging on a Flat Surface Above Leidenfrost Temperature,'' ASME J. Fluids Engineering, **118**, pp. 142–149.
[14] Hatta, N., Fujimoto, H., Kinoshita, K., and Takuda, H., 1997, ''Experimental Study of Deformation Mechanism of a Water Droplet Impinging on Hot Metallic Surfaces Above Leidenfrost Temperature,'' ASME J. Fluids Eng., **119**, pp. 692–699.
[15] Guo, T., Wang, T., and Gaddis, J. L., 2000, ''Mist/Steam Cooling in a Heated Horizontal Tube: Part 2—Results and Modeling,'' ASME J. Turbomach., **122**, pp. 366–374.
[16] Guo, T., Wang, T., and Gaddis, J. L., 2000, ''Mist/Steam Cooling in a 180-Degree Tube,'' ASME J. Heat Transfer, in press.
[17] Moffat, R. J., 1985, ''Using Uncertainty Analysis in the Planning of an Experiment,'' ASME J. Fluids Eng., **107**, pp. 173–178.
[18] Li, X., 1999, ''Cooling by a Mist/Steam Jet,'' Ph.D. Dissertation, Dept. of Mechanical Engineering, Clemson University, SC.
[19] Downs, S. J., and James, E. M., 1987, ''Jet Impingement Heat Transfer—A Literature Survey,'' ASME Paper No. 87-HT-35.
[20] Chen, J. C., and Costigan, X. Y., 1992, ''Review of Post-Dryout Heat Transfer in Dispersed Two Phase Flow,'' in: *Post-Dryout Heat Transfer*, G. F. Hewitt et al., eds., CRC Press Inc., FL, pp. 1–37.
[21] Martin, H., 1977, ''Heat and Mass Transfer Between Impinging Gas Jets and Solid Surfaces,'' Adv. Heat Transfer, **13**, pp. 1–60.
[22] Vader, D. T., Incropera, F. P., and Viskanta, R., 1991, ''Local Convective Heat Transfer From a Heated Surface to an Impinging, Planar Jet of Water,'' Int. J. Heat Mass Transf., **34**, pp. 611–623.
[23] Wolf, D. H., Viskanta, R., and Incropera, F. P., 1990, ''Local Convective Heat Transfer From a Heated Surface to a Planar Jet of Water With a Nonuniform Velocity Profile,'' ASME J. Heat Transfer, **112**, pp. 889–905.